Deformation of Nanoporous Materials in the Process of Binary Adsorption: Methane Displacement by Carbon Dioxide from Coal

Nicholas J. Corrente[1], Katarzyna Zarębska[2], and Alexander V. Neimark[1,*]

[1]Department of Chemical and Biochemical Engineering, Rutgers, The State University of New Jersey, Piscataway, NJ 08854, United States

[2]AGH University of Science and Technology, Al. Mickiewicza 30, 30-059, Krakòw, Poland

Supporting Information Placeholder

ABSTRACT: Phenomenon of adsorption-induced deformation of nanoporous materials has recently attracted a lot of attention in chemical, materials, and geoscience communities. Various theoretical and molecular simulations approaches have been suggested to predict the stress and strain induced by single component gas adsorption. Here, we develop a thermodynamic method based on the notion of the adsorption stress to predict the deformation effects upon multicomponent adsorption. As a practically important example, the process of displacement of methane by carbon dioxide from microporous carbons is considered. This process is the foundation of secondary gas recovery from shales and coalbeds associated with carbon dioxide sequestration. Theoretical predictions are correlated with the original experimental data on CO_2 and CH_4 individual and binary adsorption on coal samples coupled with *in-situ* strain measurements. With the model parameterized and verified against the experimental data at ambient conditions, the projections are made for the adsorption deformation at geological conditions of elevated pressure and temperature, which increase with the depth of the reservoir. The proposed approach may have multifaceted applications in modeling behavior of hydrocarbon mixtures in nanoporous geomaterials, gas separations and energy storage on flexible adsorbents.

I. Introduction.

The problem of predicting adsorption and deformation properties of flexible nanoporous materials has recently attracted considerable attention across various scientific disciplines, from adsorption separations and gas storage in metal-organic frameworks (MOFs) and zeolites to nanoporous drug carriers and actuators to hydrocarbon recovery and carbon dioxide sequestration in shales and coal. [1-7] The latter processes are critically important for the development of environmentally friendly energy technologies. Promising enhanced gas recovery techniques utilize injection of CO_2 to induce desorption of natural gas and simultaneous adsorption of CO_2. This process offers higher yields of natural gas, reduced pollution by eliminating wastewater, and sequestration of CO_2, a known greenhouse gas. [5, 6, 8] Geosorbents such as coals and shales are composed of poroelastic nanoporous matrices that deform significantly upon gas adsorption and desorption. [9-11] For example, organic fractions of shale have been shown to swell in excess of 20% upon adsorption of hydrocarbons. [12] Nanoporous matrix swelling causes shrinkage of the free gas pore volume and cleat spacings and significant reduction of the reservoir permeability. [13, 14]

Although the effects of adsorption-induced deformation and their practical importance are well documented for geosorbents and other nanoporous solids, most theoretical and experimental efforts are limited to single component adsorption. There are various approaches for modeling multicomponent adsorption on carbons, zeolites and MOFs that do not take into account the adsorbent deformation. [15-18] The density functional theory and Monte Carlo (MC) molecular simulation models were suggested to study adsorption-induced deformation processes on the atomistic level. [19, 20] Adsorption-induced transformations in MOFs have received a special attention. [1-3, 21-25] Several theoretical approaches have been suggested to extend the macroscopic poromechanics to nanoporous adsorbents and account for the adsorption effects. [26-32] It is worth noting the works [33-35] aimed at modeling secondary methane recovery and CO_2 sequestration on coal. The progress in theoretical modeling is hindered by a lack of systematic experimental studies of adsorbent deformation during multicomponent adsorption. Most papers report the results of either adsorption or strain measurements, but rarely both. [36-39] The comprehensive experimental data sets presented in this paper represent the unique exception.

The goal of this work is to present a rigorous thermodynamic approach to predict the adsorption-induced deformation of flexible structures upon adsorption of binary mixtures based on the information obtained from the single component measurements. In Section II, we present the general

thermodynamic foundations of the proposed approach and its implementation for the case of binary adsorption governed by the Langmuir model. Section III is devoted to the experimental methods employed for the volumetric adsorption and in-situ strain measurements upon adsorption of CH_4, CO_2, and their binary mixtures on a low rank coal. Comparison of the theory and experimental data collected at the room temperature is presented in Section IV. In Section V, predictions are made for the coal matrix swelling induced by the displacement of CH_4 by CO_2 at the geological conditions at elevated pressure and temperature. Conclusions are briefly summarized in Section VI.

II. Thermodynamics of adsorbent deformation induced by multicomponent adsorption

Deformation of a porous solid in the presence of adsorbing species is determined by the external pressure, P_{ext}, and the adsorption stress, σ_a, exerted by the guest molecules interacting with the pore walls. [19, 29] In the simplest linear elastic approximation, the volumetric strain, ε, of an isotropic solid is defined through the volumetric modulus of the solid, K, as [19]

$$\varepsilon = \frac{V-V_0}{V_0} = (\sigma_a - P_{ext})/K \qquad (1)$$

where V is the sample volume at given conditions and V_0 is the reference volume of the undeformed sample reduced per unit mass of the sample. In adsorption experiments, V_0 is the reference volume of "dry" sample evacuated at negligibly small pressures.

At the conditions of thermodynamic equilibrium between the solid and gas mixture, the adsorption stress is rigorously defined as the negative derivative of the grand thermodynamic potential of the adsorbed phase $\Omega_a(\{\mu_i\}, V, T)$ with respect to the sample volume *V,* [29]

$$\sigma_a = -\left(\frac{\partial \Omega_a}{\partial V}\right)|_{\{\mu_i\},T} \ , \qquad (2)$$

at constant temperature T and chemical potentials of the mixture components $\{\mu_i = \mu_i(\{y_i\}, p, T).\}$. The latter depend on the mixture composition (molar fractions $\{y_i\}$), pressure p and temperature T, $\mu_i = \mu_i(\{y_i\}, p, T)$. The grand thermodynamic potential of the adsorbed phase, $\Omega_a(\{\mu_i\}, V, T)$, commonly referred to in the adsorption literature as the integral work of adsorption, is related to the adsorption isotherms of mixture components, $N_i(\{\mu_i\}, V, T)$, according to the Gibbs equation,

$$d\Omega_a(\{\mu_i\}, V, T)|_{V,T} = -\sum N_i(\{\mu_i\}, V, T) d\mu_i \qquad (3)$$

The adsorption grand potential $\Omega_a(\{\mu_i\}, V, T)$ can be calculated by integration the Gibbs equation (3) along the trajectory of increasing pressure from "vacuum" at $p = 0$ to the given value p keeping the mixture composition $\{y_i\}$, sample volume, and temperature fixed,

$$\Omega_a(\{\mu_i\}, V, T) = -\int_0^p [\sum N_i^{theor}(\{\mu_i\}, V, T) \frac{\partial \mu_i}{\partial p}] dp \qquad (4)$$

Here, $N_i^{theor}(\{\mu_i\}, V, T) = N_i^{theor}(\{y_i\}, p, V, T)$ is the adsorption isotherm of component i in the mixture of composion $\{y_i\}$ at pressure p. The superscript "theor" distinguishes this theoretical isotherm from the experimental isotherm $N_i^{exp}(\{\mu_i\}, V_0, T)$ that is measured on the sample of reference volume V_0. N_i^{theor} is the absolute adsorption isotherm that represents the total adsorbed amount of component *i*, while the experimentally measured isotherm N_i^{exp} is commonly reported as the excess isotherm. [29]

Equations (1), (2), and (4) provide a general thermodynamic methodology for predicting the adsorption stress and strain induced by mixture adsorption based on the theoretical adsorption isotherms, which depend on the sample volume, V, which varies due to the deformation. The theoretical adsorption isotherms can be determined by different means, similarly as it is done for single component systems; in particular, using molecular level models of density functional theory [19, 40] and Monte Carlo simulations, [20, 41] or common phenomenological equations with parameters fitted against the experimental data, like Langmuir, [42] Dubinin-Radushkevich, [43] Derjaguin-Broekhoff-de Bour, [44] among others. Note that the sample volume, adsorption isotherms, thermodynamic potential, and other extensive characteristics can be expressed in the reduced units, as is customary in the adsorption literature, per unit mass of adsorbent. In the simulation methods, the sample volume is presented explicitly as the volume of the simulation cell, or the unit cell volume in the case of crystalline adsorbents. In the phenomenological models, the sample volume features implicitly through the physical parameters, such as adsorption capacity and adsorption energy, which depend on the sample deformation.

Let's consider the proposed general approach applied to the binary adsorption systems with the isotherms described by the conventional Langmuir model of binary adsorption,

$$N_{1/2} = \frac{N_{1/2}^0 \, K_{1/2} \, y_{1/2} \, p}{1 + K_1 y_1 p + K_2 y_2 p} \qquad (5)$$

where N_i^0 and K_i are the maximum adsorption capacity and the Henry constant, respectively, of individual component *i*=1,2. The Langmuir model is the most simple and commonly used model for description of adsorption of hydrocarbons and other light chemicals on microporous adsorbents, including adsorption of CH_4 and CO_2 on coal.[45, 46] The practical advantage of the Langmuir model is that it depends on the physical parameters, N_i^0 and K_i, which vary with the alteration of the sample volume affected by deformation. At

the same time, it is oversimplistic and has apparent limitations; it implies the ideal gas phase and ignores the pore size distribution and surface energy heterogeneity.

Noteworthy, the Henry constants K_i depend on the energy of adsorption and decrease with temperature following the van't Hoff equation,

$$K_i(T) \sim exp\left[-\frac{\Delta H_i}{RT}\right], \qquad (6)$$

where ΔH_i is the equilibrium enthalpy of adsorption of species i.[47] Equation (6) allows for prediction of the temperature dependence of the adsorption and strain isotherms, as shown below.

For the Langmuir model (5), the integral in Eq. 4 is calculated explicitly. In case of a binary ideal gas mixture implied by the Langmuir model (5), the chemical potential of the individual components is equal to $\mu_i = RTln(y_i p)$, and Equation (4) is given in a simple form,

$$\Omega_a = -RT \int_0^p [N_1(y_1, y_2, p, V, T) + N_2(y_1, y_2, p, V, T)] \frac{1}{p} dp \qquad (7)$$

For the Langmuir model (5), the grand thermodynamic potential (7) reduces to the following simple relationship,

$$\Omega_a = -\frac{RT\left(K_1 N_1^0 y_1 + K_2 N_2^0 y_2\right) ln(1+K_1 y_1 p + K_2 y_2 p)}{K_1 y_1 + K_2 y_2} \qquad (8)$$

Consequently, the adsorption stress (2) is determined by direct differentiation of Equation (8), as

$$\sigma_a = -\left(\frac{\partial \Omega_a}{\partial N_1^0}\frac{\partial N_1^0}{\partial V} + \frac{\partial \Omega_a}{\partial N_2^0}\frac{\partial N_2^0}{\partial V} + \frac{\partial \Omega_a}{\partial K_1}\frac{\partial K_1}{\partial V} + \frac{\partial \Omega_a}{\partial K_2}\frac{\partial K_2}{\partial V}\right) = \frac{RTK_1 y_1 ln(1+K_1 p_1 + K_2 p_2)}{K_1 y_1 + K_2 y_2}\frac{\partial N_1^0}{\partial V} + \frac{RTK_2 y_2 ln(1+K_1 p_1 + K_2 p_2)}{K_1 y_1 + K_2 y_2}\frac{\partial N_2^0}{\partial V} + \frac{RTy_1\left(\frac{p(K_1 y_1 + K_2 y_2)\left(K_1 N_1^0 y_1 + K_2 N_2^0 y_2\right)}{1+K_1 p_1 + K_2 p_2}\right)}{(K_1 y_1 + K_2 y_2)^2}\frac{\partial K_1}{\partial V} + \frac{RTy_1\left(K_2 y_2\left(N_1^0 - N_2^0\right) ln(1+K_1 p_1 + K_2 p_2)\right)}{(K_1 y_1 + K_2 y_2)^2}\frac{\partial K_1}{\partial V} + \frac{RTy_2\left(\frac{p(K_1 y_1 + K_2 y_2)\left(K_1 N_1^0 y_1 + K_2 N_2^0 y_2\right)}{1+K_1 p_1 + K_2 p_2}\right)}{(K_1 y_1 + K_2 y_2)^2}\frac{\partial K_2}{\partial V} + \frac{RTy_2\left(K_1 y_1\left(N_2^0 - N_1^0\right) ln(1+K_1 p_1 + K_2 p_2)\right)}{(K_1 y_1 + K_2 y_2)^2}\frac{\partial K_2}{\partial V} \qquad (9)$$

Here, $\frac{\partial N_{1/2}^0}{\partial V}$ represents the change in the maximum adsorption capacity with the variation of the sample volume, and $\frac{\partial K_{1/2}}{\partial V}$ is related to the respective change in the energy of adsorption according to Equation 6. The adsorption stress for pure component adsorption can be found from Equation (8) by setting the respective mole fraction y_i=1

$$\sigma_{a,i} = RT\left[\frac{N_{1/2}^0 p}{1+K_{1/2}p}\frac{\partial K_{1/2}}{\partial V} + ln\left(1+K_{1/2}p\right)\frac{\partial N_{1/2}^0}{\partial V}\right] \qquad (10)$$

Noteworthy, Equation (10) for single component adsorption was derived and employed earlier for modeling breathing transitions in MIL-53 MOFs. [42]

For further analysis, it is useful to introduce the dimensionless parameters, which represent the capacity and Henry constant susceptibility factors, $\lambda_{N_{1/2}^0} = \frac{\partial N_{1/2}^0}{\partial V}\frac{V_0}{N_{1/2}^0(V_0)}$ and $\lambda_{K_{1/2}} = \frac{\partial K_{1/2}}{\partial V}\frac{V_0}{K_{1/2}(V_0)}$. The susceptibility factors, $\lambda_{N_{1/2}^0}$ and $\lambda_{K_{1/2}}$, show the percentage of the adsorption capacity and Henry constant changes induced by the volumetric strain of 1%.

Equations (5) and (9) allows for the prediction of the adsorption isotherm and stress in the process of binary adsorption at different mixture compositions, pressures and temperatures based on the experimental data on pure component adsorption measured at one temperature. To this end, the adsorption capacities and Henry constant, N_i^0 and K_i, and their susceptibility factors, $\lambda_{N_i^0}$ and λ_{K_i}, are determined from the experimental pure component adsorption and strain isotherms, respectively. The adsorption isotherms are fitted by the single component Langmuir equation (Equation (5) with y_1 =1, 0) to determine N_i^0 and K_i. The pure component strain isotherms are fitted by Equation (1) with the adsorption stress $\sigma_{a,i}$ given by Equation (10); external pressure in gas adsorption experiment is equal to the gas pressure, $P_{ext} = p$.

III. In-situ measurements of coal deformation during CO_2 and CH_4 adsorption.

In order to illustrate the proposed approach, we consider adsorption of pure CH_4 and CO_2 and their mixture on low rank coal at the room temperature 298 K. Sorption and deformation measurements were taken using the specially designed home-made apparatus described in refs. [48]. The system comprises a low-pressure (glass) dosing unit used for degassing and calibration and a high-pressure ampoule (made of metal), which enables the gas sorption tests in the elevated pressures by the volumetric method. The pressure is monitored over the range 0–4.0 MPa with an accuracy of ±1 kPa. The system was assumed to be at a near-equilibrium state when the pressure variations in the ampoule fell within ±2 kPa. The in-situ deformation measurements during adsorption of pure CH_4 and CO_2 and their mixture is performed by tensiometers affixed to the surface of the coal sample placed in the high-pressure ampoule. Variation of the sample strain

is determined from the strain gauge resistances measured by the compensating method, using the Wheatstone's bridge

Repeated measurements are performed with increasing pressures in the dosing unit. The composition of the gas mixture in the ampoule is measured with a gas chromatograph after the final pressure measurement is obtained. The detailed conditions of the experiments are described in earlier papers. [45, 48]

Below, we use the experimental data collected on two samples from the Brzeszcze coal mine in the Upper Silesia Coal Basin, denotated B32.2 and B32.1. For sample B32.2, the mixture experiments were performed for two compositions of 27% and 75% carbon dioxide. The mixture adsorption and strain experimental data for 27% and 75% CO_2 feed composition correspond to the CO_2 fraction in equilibrated gas phase of 14.2% and 57.5%, respectively, at the highest pressure. We use the recalibrated the raw data on adsorption and strain isotherms reported separately in Refs. [48, 49] During recalibration, the CO_2 fractions for lower pressure were estimated using the material balances (for details see Supplementary Information, Section 1).

For sample B32.1, the adsorption isotherms and pure CH_4 and mixture strain isotherms were reported earlier in Refs. [45, 46], while the pure CO_2 strain isotherm on this sample is presented here for the first time. The mixture experiments were performed with the feeding mixture of 41.5% CO_2 that corresponded to the 23.4 CO_2 fraction in equilibrated gas phase at the highest pressure.

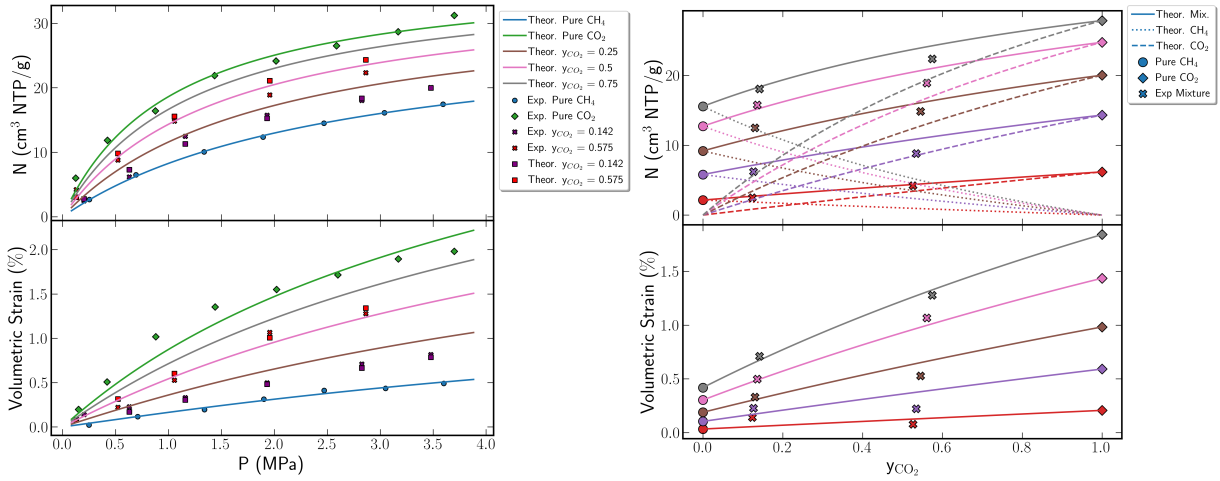

Figure 1. Left: Adsorption (upper) and strain (lower) isotherms for pure carbon dioxide (green), pure methane (blue), and binary mixtures (red, purple) on coal sample B32.2. Green points represent experimental pure CO_2 data, blue points represent pure CH_4 data, red and purple crosses represent experimental mixture data, and lines and red and purple squares represent pure species and mixture predictions, respectively from Eqs. (5) and (9). Right: Prediction of the variation of adsorption and strain as functions of the estimated CO_2 fractions, y_{CO2}, in the process of displacement of CH_4 by CO_2 at various gas pressures. Experimental data points correspond to pure CO_2 (diamonds) and CH_4 (circles) at y_{CO2} = 0,1, and mixtures (crosses) at the CO_2 fractions estimated from material balances; the left set corresponds to the final y_{CO2} = 0.142, and the right corresponds to y_{CO2} = 0.575. Predictions for the mixtures (solid lines) and pure CO_2 and CH_4 (dashed and dotted lines, respectively) are calculated at pressures of 0.203 MPa (red), 0.63 MPa (purple), 1.158 MPa (brown), 1.931 MPa (pink), and 2.825 MPa (grey). The strain is counted from the reference "dry" state of the adsorbent at P=0.

IV. Correlation of theory and experiments

Figure 1 illustrates the application of the proposed methodology. The left panel shows the correlation of the theoretical predictions with the experimental adsorption and *in-situ* strain data for pure carbon dioxide and methane and their binary mixtures on sample B32.2 at the room temperature 298 K. The set of model parameters, N_i^0, K_i, $\lambda_{N_i^0}$ and λ_{K_i}, fitted to reproduce the pure component measurements is listed in Table 1.

Table 1. Model parameters for sample B32.2 determined from the pure component adsorption and strain isotherms.

	K_i, MPa−1	N_i^0, cm3 NTP/g	$\lambda_{K_{1/2}}$, %	$\lambda_{N_i^0}$, %
CO2	0.951	38.2	-0.386	0.943
CH4	0.380	30.1	-0.429	0.772

For the conversion of the calculated adsorption stress into the strain, the volumetric modulus, K, is taken as 2 GPa, which is typical for coals. [50] The theoretical adsorption and strain isotherms for pure components calculated with fitted parameters agree reasonably with the experimental data. As expected, CO_2 adsorption is stronger than CH_4 adsorption that is characterized by larger adsorption capacity and larger adsorption stress and strain. This trend was found in other

similar systems. [5, 6] At sufficiently low pressures, the strain is negative meaning that the sample contracts upon adsorption. Although the contraction effect is small, this behavior is typical for all microporous adsorbents, including carbons, zeolites and MOFs. [19, 42, 43] Contraction at low gas pressures is accounted for by the negative Henry constant susceptibility factor, $\lambda_{K_{1/2}}$ (see Table 1), that is related according to Equation (6) to the change of the adsorption energy with the pore size, $\lambda_{K_{1/2}} \approx -\frac{\partial \Delta H_i/\partial V}{RT}$: the smaller the pore, the larger the adsorption energy, ΔH_i. This effect leads to the negative adsorption stress exerted on the pore walls that tends to pull them inward. With further increase of pressure and adsorbate density, the repulsion between adsorbed molecules causes the positive stress that tends to push against the pore walls and leads to swelling. For adsorption in this sample the contraction effect was not revealed in the experiments, as it likely occurs at lower pressures than those measured. However, it is visible for CH_4 adsorption on sample B32.1 (see Figure S2 in Supplementary Information).

Predicted mixture adsorption and strain isotherms gradually increase as the CO_2 fraction, y_{CO2}, increases. The experimental data (limited to the range of y_{CO2}=0.091-0.156 and y_{CO2}=0.575-0.628 for each feed mixture) agree with the theoretical predictions within acceptable deviations. These deviations are likely due to the experimental uncertainty in the gas composition measurements.

The model developed allows for theoretical predictions of the variation of the adsorption and strain in the process of displacement of CH_4 by CO_2. The respective adsorption and strain isotherms as functions of the CO_2 fraction, y_{CO2}, at the selected fixed gas pressures at 298 K, are shown in the right panel of Figure 1. As expected, due to a higher affinity of CO_2 to carbon, the total gas adsorption gradually increases between the values of pure component CH_4 and CO_2 adsorption at given pressure. Respectively, the strain measured from the initial volume of the sample saturated with pure CH_4 increases monotonically, which reflects swelling of the coal upon the CH_4 displacement by CO_2. The available experimental data for two mixture compositions, $y_{CO2} = 0.142$ and $y_{CO2} = 0.575$, are correlated with the theoretical predictions.

Similar calculations compared with experimental data for sample B32.1 are presented in Supplementary Information, Section 3.

V. Prediction of coal deformation during CH_4 displacement by CO_2 at geological conditions

It is of practical interest to estimate the effects of coal swelling at the geologically relevant conditions, [51, 52] where both temperature and pressure increase with the depth of the gas reservoir. The interpolation to the higher temperature is done with the van't Hoff equation (6). For the given sample, the enthalpy of CO_2 adsorption, $\Delta H_{CO2} = -36.911 kJ/mol$, was determined from the isotherms measured at 298 K and 323 K. For CH_4 adsorption, we used the enthalpy $\Delta H_{CH4} = -33.4 kJ/mol$ reported in ref. [53] for a similar coal sample. Equation (6) is also used to recalculate the Henry constant susceptibility factor as a function of temperature, $\lambda_{K_{1/2}} \sim 1/T$.

Calculations of the adsorption and strain were performed for the coal sample B32.2 that would be placed at different depths below the surface level at 0 m (T=298K, P=0.1 MPa), 500 m (T=313K, P=5.1 MPa), 1,000 m (T=328K, P=10.1 MPa), 1,500 m (T=343K, P=15.1 MPa), and 2,000 m (T=358K, P=20.1 MPa). With the depth of the reservoir, pure component adsorption and sample deformation dependencies are nonmonotonic, as shown in Figure 2, left panel. The respective values of temperature and pressure are given in the figure. The nonmonotonic behavior is caused by a competition between the pressure and temperature effects, which act in opposite directions, [36] see more details in Supplementary Information, Section 2. Pure component adsorption and strain sharply increase with the depth up to 500 m due to the pressure increase by an order of magnitude. However, further increase of pressure in the diapason of depths 1,000-2,000 m is compensated by the rise of temperature, and the adsorption reaches a near plateau at about 14 cm^3 NTP/g and 25.5 cm^3 NTP/g for CH_4 and CO_2, respectively. Therewith, the adsorption induced strain decreases for the pure components at the depths below 500 m. The non-monotonic behavior of the strain with the depth of the reservoir is attributed to the negative Henry constant susceptibility factor, $\lambda_{K_{1/2}}$, as shown in Supplementary Information, Section 2 Figure S1. Note that here the strain is counted from the reference state of the "dry" adsorbent at T=298K and P=0. The strain induced due to the complete CH_4 displacement by CO_2 is estimated as the difference in the strain for pure components (green data on Fig. 2, left), which increases with the reservoir depth achieving a plateau below 500 m. The resulting swelling is estimated about 1.25%.

The right panel of Figure 2 depicts the calculated adsorption and strain isotherms as functions of the bulk CO_2 mole fraction during the process of CH_4 displacement by CO_2 assuming the constant temperature and pressure corresponding to the given depths below the surface level. The adsorption strain is counted from the strain of the sample saturated by pure CH_4 to demonstrate the effect of CH_4 displacement by CO_2. The theoretical predictions suggest that coal swelling due to CH_4 displacement by CO_2 is progressively

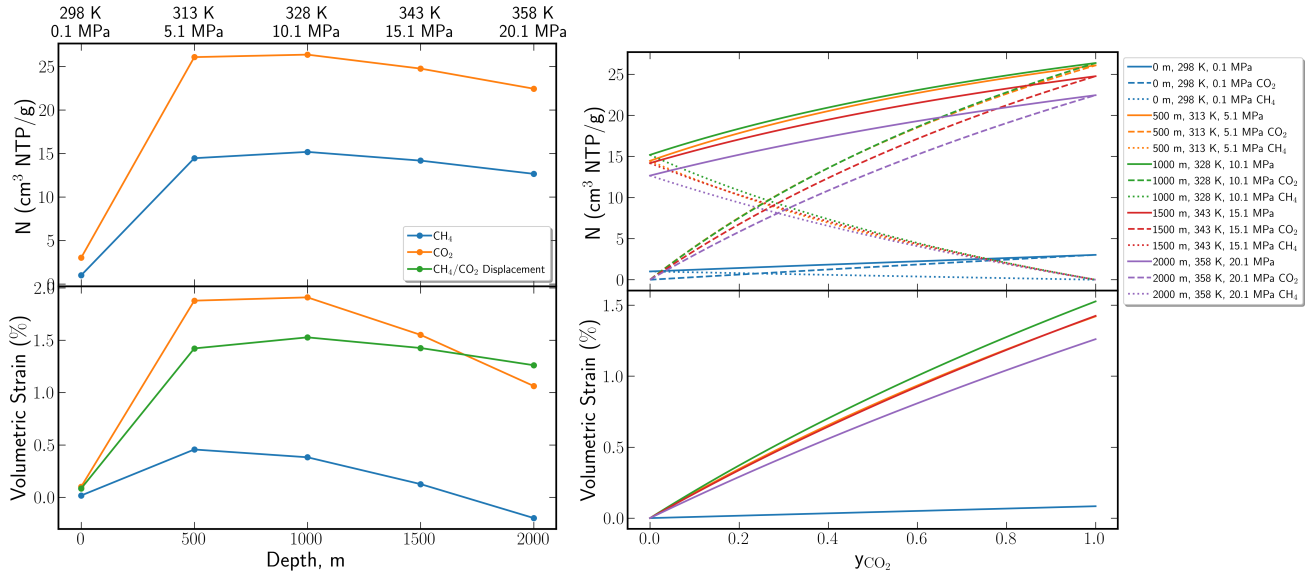

Figure 2: Prediction of adsorption and deformation upon the displacement of CH_4 by CO_2 at geological conditions at the levels of 0, 500, 1,000, 1,500, and 2,000 m below the surface. Left: Adsorption and strain of the coal sample with pure CH_4 and CO_2 at geological conditions. The strain is counted from the reference state of the "dry" adsorbent at T=298K and P=0. The strain difference due to the complete displacement of CH_4 by CO_2 is shown in green. Right: Adsorption (upper) and strain (lower) isotherms as a function of bulk CO_2 fraction, y_{CO2}, and the respective pressure and temperature shown in the figure caption. Solid, dotted, and dashed lines represent respectively the total adsorption and strain, CH_4 and CO_2 adsorption. The strain is counted from the state of the adsorbent saturated by pure CH_4 at given pressure.

pronounced with the depth of the reservoir, reaching approximately 1.55% volumetric strain at a depth of 1000 m and decreasing slightly with the depth at 1,500 m and below. This nonmonotonic effect is due to the initial elevated underearth pressure and respectively enhanced adsorption of both CH_4 and CO_2, with the latter having a stronger affinity to coal. At increasing depths above 1000 m, the effect of the increase in temperature overcomes the pressure enhancement, and the strain and adsorption decrease with increasing depth.

Similar calculations for sample B32.1 showing the same trends are presented in Supplementary Information, Section 3, Figure S3.

VI. Conclusions.

The proposed adsorption stress theory allows for predicting the deformation of nanoporous materials induced by adsorption of gas mixtures based on the experimental data for pure gas mixture components. Using the Langmuir adsorption model, we demonstrate the correlation of the theoretical predictions with the experimental adsorption and strain data for pure CO_2, CH_4, and their binary mixtures on the coal samples at ambient temperature.

The model parameterized based on the experimental data on pure component adsorption at ambient conditions is further employed for evaluating swelling of coal in the process of displacement of CH_4 by CO_2 geosorbents at the geological conditions. In the absence of relevant experimental data, these theoretical predictions may have important implications for the CO_2 assisted secondary gas recovery and CO_2 sequestration in geological reservoirs.

It should be noted that while the Langmuir model is widely used for description of binary adsorption on various microporous materials, it has apparent limitations. The proposed general approach requires the knowledge of the theoretical adsorption isotherms, which can be determined by various methods including more complex phenomenological adsorption models, or direct MC and DFT simulations of gas adsorption on model solid structures. With proper modifications, the proposed approach can be extended and applied for other practical applications, including various gas mixture separation processes on flexible nanoporous adsorbents, like zeolites and MOFs.

ASSOCIATED CONTENT

Supporting Information.
The Supporting Information is available free of charge on the ACS Publications website. It includes: estimation of the CO_2 fraction in the equilibrium gas phase during adsorption measurements; model predictions at geological conditions; and comparison of the theoretical predictions and experimental data for sample B32.1 (PDF).

AUTHOR INFORMATION

Corresponding Author

*aneimark@rutgers.edu (A.V. Neimark)

ACKNOWLEDGMENT

This work is supported by the National Science Foundation (CBET grant No. 18334339).

REFERENCES

1. Coudert, F. o.-X.; Boutin, A.; Fuchs, A. H.; Neimark, A. V., Adsorption deformation and structural transitions in metal–organic frameworks: from the unit cell to the crystal. *The Journal of Physical Chemistry Letters* **2013,** *4* (19), 3198-3205.

2. Agrawal, M.; Bhattacharyya, S.; Huang, Y.; Jayachandrababu, K. C.; Murdock, C. R.; Bentley, J. A.; Rivas-Cardona, A.; Mertens, M. M.; Walton, K. S.; Sholl, D. S., Liquid-phase multicomponent adsorption and separation of xylene mixtures by flexible MIL-53 adsorbents. *The Journal of Physical Chemistry C* **2018,** *122* (1), 386-397.

3. Taylor, M. K.; Runčevski, T. e.; Oktawiec, J.; Bachman, J. E.; Siegelman, R. L.; Jiang, H.; Mason, J. A.; Tarver, J. D.; Long, J. R., Near-perfect CO2/CH4 selectivity achieved through reversible guest templating in the flexible metal–organic framework Co (bdp). *Journal of the American Chemical Society* **2018,** *140* (32), 10324-10331.

4. Lin, J.-L.; Wang, Z.-K.; Xu, Z.-Y.; Wei, L.; Zhang, Y.-C.; Wang, H.; Zhang, D.-W.; Zhou, W.; Zhang, Y.-B.; Liu, Y., Water-soluble flexible organic frameworks that include and deliver proteins. *Journal of the American Chemical Society* **2020,** *142* (7), 3577-3582.

5. Klewiah, I.; Berawala, D. S.; Walker, H. C. A.; Andersen, P. Ø.; Nadeau, P. H., Review of experimental sorption studies of CO2 and CH4 in shales. *Journal of Natural Gas Science and Engineering* **2020,** *73*, 103045.

6. Iddphonce, R.; Wang, J.; Zhao, L., Review of CO2 injection techniques for enhanced shale gas recovery: Prospect and challenges. *Journal of Natural Gas Science and Engineering* **2020,** *77*, 103240.

7. Schneemann, A.; Bon, V.; Schwedler, I.; Senkovska, I.; Kaskel, S.; Fischer, R. A., Flexible metal–organic frameworks. *Chemical Society Reviews* **2014,** *43* (16), 6062-6096.

8. Mukherjee, M.; Misra, S., A review of experimental research on Enhanced Coal Bed Methane (ECBM) recovery via CO2 sequestration. *Earth-Science Reviews* **2018,** *179*, 392-410.

9. Huang, L.; Ning, Z.; Wang, Q.; Qi, R.; Cheng, Z.; Wu, X.; Zhang, W.; Qin, H., Molecular insights into kerogen deformation induced by CO2/CH4 sorption: effect of maturity and moisture. *Energy & Fuels* **2019,** *33* (6), 4792-4805.

10. Huang, L.; Ning, Z.; Wang, Q.; Qi, R.; Cheng, Z.; Wu, X.; Zhang, W.; Qin, H., Kerogen deformation upon CO2/CH4 competitive sorption: Implications for CO2 sequestration and enhanced CH4 recovery. *Journal of Petroleum Science and Engineering* **2019,** *183*, 106460.

11. Bakhshian, S.; Sahimi, M., Adsorption-induced swelling of porous media. *International Journal of Greenhouse Gas Control* **2017,** *57*, 1-13.

12. Ertas, D.; Kelemen, S. R.; Halsey, T. C., Petroleum expulsion part 1. Theory of kerogen swelling in multicomponent solvents. *Energy & Fuels* **2006,** *20* (1), 295-300.

13. Pang, Y.; Chen, S.; Soliman, M. Y.; Morse, S. M.; Hu, X., Evaluation of matrix swelling behavior in shale induced by methane sorption under triaxial stress and strain conditions. *Energy & Fuels* **2019,** *33* (6), 4986-5000.

14. Xue, S.; Zheng, C.; Kizil, M.; Jiang, B.; Wang, Z.; Tang, M.; Chen, Z., Coal permeability models for enhancing performance of clean gas drainage: A review. *Journal of Petroleum Science and Engineering* **2021**, 108283.

15. Myers, A., Thermodynamics of adsorption in porous materials. *AIChE Journal* **2002,** *48* (1), 145-160.

16. Myers, A.; Monson, P., Adsorption in porous materials at high pressure: theory and experiment. *Langmuir* **2002,** *18* (26), 10261-10273.

17. Krishna, R.; van Baten, J. M., How Reliable Is the Ideal Adsorbed Solution Theory for the Estimation of Mixture Separation Selectivities in Microporous Crystalline Adsorbents? *ACS Omega* **2021**.

18. Fraux, G.; Boutin, A.; Fuchs, A. H.; Coudert, F.-X., On the use of the IAST method for gas separation studies in porous materials with gate-opening behavior. *Adsorption* **2018,** *24* (3), 233-241.

19. Ravikovitch, P. I.; Neimark, A. V., Density functional theory model of adsorption deformation. *Langmuir* **2006,** *22* (26), 10864-10868.

20. Kowalczyk, P.; Ciach, A.; Neimark, A. V., Adsorption-induced deformation of microporous carbons: Pore size distribution effect. *Langmuir* **2008,** *24* (13), 6603-6608.

21. Goeminne, R.; Krause, S.; Kaskel, S.; Verstraelen, T.; Evans, J. D., Charting the Complete Thermodynamic Landscape of Gas Adsorption for a Responsive Metal–Organic Framework. *Journal of the American Chemical Society* **2021,** *143* (11), 4143-4147.

22. Bakhshian, S.; Sahimi, M., Theoretical model and numerical simulation of adsorption and deformation in flexible metal–organic frameworks. *The Journal of Physical Chemistry C* **2018,** *122* (17), 9465-9473.

23. Maurin, G.; Serre, C.; Cooper, A.; Férey, G., The new age of MOFs and of their porous-related solids. *Chemical Society Reviews* **2017,** *46* (11), 3104-3107.

24. Krause, S.; Evans, J. D.; Bon, V.; Senkovska, I.; Ehrling, S.; Iacomi, P.; Többens, D. M.; Wallacher, D.; Weiss, M. S.; Zheng, B., Engineering micromechanics of soft porous crystals for negative gas adsorption. *Chemical science* **2020,** *11* (35), 9468-9479.

25. Formalik, F.; Neimark, A. V.; Rogacka, J.; Firlej, L.; Kuchta, B., Pore opening and breathing transitions in metal-organic frameworks: Coupling adsorption and deformation. *Journal of Colloid and Interface Science* **2020,** *578*, 77-88.

26. Vandamme, M., Coupling between adsorption and mechanics (and vice versa). *Current Opinion in Chemical Engineering* **2019,** *24*, 12-18.

27. Chen, M.; Coasne, B.; Guyer, R.; Derome, D.; Carmeliet, J., A Poromechanical Model for Sorption Hysteresis in Nanoporous Polymers. *The Journal of Physical Chemistry B* **2020,** *124* (39), 8690-8703.

28. Le, T. D.; Moyne, C.; Murad, M. A.; Panfilova, I., A three-scale poromechanical model for swelling porous media incorporating solvation forces: Application to enhanced coalbed methane recovery. *Mechanics of Materials* **2019,** *131*, 47-60.

29. Neimark, A. V., Reconciliation of Gibbs Excess Adsorption Thermodynamics and Poromechanics of Nanoporous Materials. In *Poromechanics VI*, 2017; pp 56-63.

30. Coasne, B.; Weigel, C.; Polian, A.; Kint, M.; Rouquette, J.; Haines, J.; Foret, M.; Vacher, R.; Rufflé, B., Poroelastic theory applied to the adsorption-induced deformation of vitreous silica. *The Journal of Physical Chemistry B* **2014,** *118* (49), 14519-14525.

31. Espinoza, D.; Vandamme, M.; Dangla, P.; Pereira, J.-M.; Vidal-Gilbert, S., Adsorptive-mechanical properties of reconstituted granular coal: Experimental characterization and poromechanical modeling. *International Journal of Coal Geology* **2016,** *162*, 158-168.

32. Espinoza, D. N.; Vandamme, M.; Pereira, J.-M.; Dangla, P.; Vidal-Gilbert, S., Measurement and modeling of adsorptive–poromechanical properties of bituminous coal cores exposed to CO2: Adsorption, swelling strains, swelling stresses and impact on fracture permeability. *International Journal of Coal Geology* **2014,** *134*, 80-95.

33. Le, T. D.; Ha, Q. D.; Panfilov, I.; Moyne, C., Multiscale model for flow and transport in CO2-enhanced coalbed methane recovery incorporating gas mixture adsorption effects. *Advances in Water Resources* **2020,** *144*, 103706.

34. Nikoosokhan, S.; Vandamme, M.; Dangla, P., A poromechanical model for coal seams saturated with binary mixtures of CH4 and CO2. *Journal of the Mechanics and Physics of Solids* **2014,** *71*, 97-111.

35. Brochard, L.; Vandamme, M.; Pellenq, R. J.-M.; Fen-Chong, T., Adsorption-induced deformation of microporous materials: coal swelling

induced by CO2–CH4 competitive adsorption. *Langmuir* **2012,** *28* (5), 2659-2670.

36. Baran, P.; Czerw, K.; Czuma, N.; Zarębska, K.; Ćwik, A., Development of temperature-induced strains in coal–CH4 and coal–CO2 systems. *Adsorption Science & Technology* **2019,** *37* (1-2), 24-33.

37. Baran, P.; Czerw, K.; Samojeden, B.; Czuma, N.; Zarębska, K., The influence of temperature on the expansion of a hard coal-gas system. *Energies* **2018,** *11* (10), 2735.

38. Heuchel, M.; Davies, G.; Buss, E.; Seaton, N., Adsorption of carbon dioxide and methane and their mixtures on an activated carbon: simulation and experiment. *Langmuir* **1999,** *15* (25), 8695-8705.

39. Liu, S.; Wang, Y.; Harpalani, S., Anisotropy characteristics of coal shrinkage/swelling and its impact on coal permeability evolution with CO2 injection. *Greenhouse Gases: Science and Technology* **2016,** *6* (5), 615-632.

40. Liu, J.; Xi, S.; Chapman, W. G., Competitive sorption of CO2 with gas mixtures in nanoporous shale for enhanced gas recovery from density functional theory. *Langmuir* **2019,** *35* (24), 8144-8158.

41. Cornette, V.; de Oliveira, J. A.; Yelpo, V.; Azevedo, D.; López, R. H., Binary gas mixture adsorption-induced deformation of microporous carbons by Monte Carlo simulation. *Journal of colloid and interface science* **2018,** *522*, 291-298.

42. Neimark, A. V.; Coudert, F.-X.; Boutin, A.; Fuchs, A. H., Stress-based model for the breathing of metal– organic frameworks. *The journal of physical chemistry letters* **2010,** *1* (1), 445-449.

43. Neimark, A. V.; Grenev, I., Adsorption-Induced Deformation of Microporous Solids: A New Insight from a Century-Old Theory. *The Journal of Physical Chemistry C* **2019,** *124* (1), 749-755.

44. Balzer, C.; Waag, A. M.; Putz, F.; Huesing, N.; Paris, O.; Gor, G. Y.; Neimark, A. V.; Reichenauer, G., Mechanical Characterization of Hierarchical Structured Porous Silica by in Situ Dilatometry Measurements during Gas Adsorption. *Langmuir* **2019,** *35* (8), 2948-2956.

45. Ceglarska-Stefańska, G.; Zarębska, K., Expansion and contraction of variable rank coals during the exchange sorption of CO2 and CH4. *Adsorption Science & Technology* **2002,** *20* (1), 49-62.

46. Ceglarska-Stefańska, G.; Zarębska, K., Sorption of carbon dioxide–methane mixtures. *International Journal of Coal Geology* **2005,** *62* (4), 211-222.

47. Du, X.; Cheng, Y.; Liu, Z.; Yin, H.; Wu, T.; Huo, L.; Shu, C., CO2 and CH4 adsorption on different rank coals: A thermodynamics study of surface potential, Gibbs free energy change and entropy loss. *Fuel* **2021,** *283*, 118886.

48. Zarębska, K.; Ceglarska-Stefańska, G., The change in effective stress associated with swelling during carbon dioxide sequestration on natural gas recovery. *International Journal of Coal Geology* **2008,** *74* (3-4), 167-174.

49. Ceglarska-Stefańska, G.; Zarębska, K.; Wolszczak, J., Sorption of pure components and mixtures CO2 and CH4 on hard coals. *Gospodarka Surowcami Mineralnymi* **2008,** *24* (4/1), 123-131.

50. Levine, J. R., Model study of the influence of matrix shrinkage on absolute permeability of coal bed reservoirs. *Geological Society, London, Special Publications* **1996,** *109* (1), 197-212.

51. Yang, K.; Lu, X.; Lin, Y.; Neimark, A. V., Deformation of coal induced by methane adsorption at geological conditions. *Energy & fuels* **2010,** *24* (11), 5955-5964.

52. Yang, K.; Lu, X.; Lin, Y.; Neimark, A. V., Effects of CO2 adsorption on coal deformation during geological sequestration. *Journal of Geophysical Research: Solid Earth* **2011,** *116* (B8).

53. Zhou, L.; FENG, Q.-Y.; Qin, Y., Thermodynamic analysis of competitive adsorption of CO2and CH4on coal matrix. *Journal of China Coal Society* **2011,** *36* (8), 1307-1311.

Table of Contents Graphics